Pakistan J. Zool., pp 1-10, 2022. **DOI**: https://dx.doi.org/10.17582/journal.pjz/20210728090730

Identification of ADPKD-Related Key miRNAs by Constructing a miRNA-mRNA Interaction Network and Experimental Verification

Hui Fang*, Kai Xue and Teng Yang

School of Pharmacy, Weifang Medical University, Weifang 261053, Shandong, China.

ABSTRACT

There are many physiological processes that rely on the microRNA-messenger RNA (miRNA-mRNA) network. In this study, an analysis of miRNA-mRNA networks was conducted to identify miRNAs linked to autosomal dominant polycystic kidney disease (ADPKD). Fifty RNA samples from Gene Expression Omnibus (GEO) database were obtained to identify differentially expressed miRNAs (DEMs) and genes (DEGs) in the progression of ADPKD. Functional annotation and enrichment analysis of DEG were performed. iRegulon was used to construct the miRNA-mRNA network and predict related transcription factors (TFs) associated with ADPKD. The function of miRNA network was explored by analyzing GO and KEGG enrichment. Further, qRT-PCR was performed *in vitro* to determine the expression of miRNAs and mRNAs associated with ADPKD. In the results, 2 DEMs and 1090 DEGs were identified. While DEGs that were downregulated tended to be enriched for metabolic pathways, DEGs that were upregulated tended to be enriched for beta-alanine metabolism, alanine, aspartate, and glutamate metabolism. The miRNA-mRNA network consisted of 2 miRNAs (miR-199a-3p and miR-107) and 7 mRNAs. It appears that miRNAs may positively regulate fibroblast migration, calcium signaling, and cell division based on GO and KEGG analysis. What's more, by detecting the expression of the key ADPKD-related miRNA-mRNA in vitro experiments, two miRNAs (miR-199a-3p, miR-107) and four candidate target mRNAs (Protein Kinase C Epsilon, PRKCE; Transmembrane P24 Trafficking Protein 5, TMED5; RUNX1 Partner Transcriptional Co-Repressor 1, RUNX1T1; and Fibroblast growth factor 2, FGF2) were identified. In conclusion, ADPKD may be better understood by examining the novel miRNA-mRNA network we constructed.

Article Information
Received 28 July 2021
Revised 14 September 2022
Accepted 01 October 2022
Available online 09 November 2022 (early access)

Authors' Contribution
Methodology and validation: TY. Conceptualization, formal analysis: HF and TY. Investigation and data curation: KX. Writing-original draft reparation: HF and KX. Writing review and editing, project administration, supervision: HF. All authors have read and agreed to the published version of the manuscript.

Key words
Kidney, ADPKD, Biomarkers, miRNA-mRNA, DEMs, DEGs, Bioinformatic analysis

INTRODUCTION

One of the most common hereditary renal diseases, autosomal dominant polycystic kidney disease (ADPKD) is caused by mutations in the *PKD1* gene (85% of cases) or in the *PKD2* gene (the remaining 15% of cases) involving multiple cell signaling pathways. About 12.5 million people worldwide suffer from this life-threatening end-stage kidney disease (Cornec-Le-Gall *et al*., 2019). Typical characteristics of ADPKD are the destruction of normal renal parenchyma, hypertension, and relentless progressive development of fluid-filled kidney cysts (Nobakht *et al*., 2020). Aside from hemodialysis or kidney transplantation, ADPKD is treated by decreasing cyclic adenosine monophosphate levels (cAMP) and preventing abnormal cell proliferation (Cornec-Le-Gall *et al*., 2019). In recent decades, numerous preclinical and clinical studies have been conducted to reveal the mechanisms of ADPKD, such as mammalian target of rapamycin (MTOR) activation (Gevers and Drenth, 2011; Song *et al*., 2021), Notch (Idowu *et al*., 2018; Radadiya *et al*., 2021), peroxisome proliferator-activated receptor α (PPARα) (Lakhia, 2020, 2018) signaling, and pathways associated with fibrosis in addition to janus kinases and signal transducers, Wnt, Wnt-like, and nuclear factor kappa-B (NF-κB) molecules participate in transcription (Xue and Mei, 2019). There are currently no reliable and effective treatments for this disease, so the creation of new therapeutic approaches is imperative (Xu *et al*., 2017). However, the pathogenesis of ADPKD is complex involving many different mechanisms and has not been fully elucidated (Shen *et al*., 2020).

microRNA (miRNA) suppresses protein synthesis through suppressing messenger RNA (mRNA) translation by binding particular regions of mRNA (Bai *et al*., 2018). As mature miRNAs, they direct the post-transcriptional

* Corresponding author: fanghui8@wfmc.edu.cn
0030-9923/2022/0001-0001 $ 9.00/0

repression of their mRNA targets, by inhibiting translation or targeting degradation of mRNA (Kotani *et al*., 2009). So, miRNAs regulate hundreds of proteins' transcriptional expression levels and each mRNA contains a different miRNA response element, so more than one miRNA might target the same mRNA (Shi *et al*., 2020). The function of the miRNA carried by the ADPKD is yet to be defined. The altered expression of miRNA may play an important role in ADPKD pathogenesis. Thus, developing anti-miRNA drugs targeting miRNA as therapeutics is feasible (Yheskel and Patel, 2017). miRNA could play an essential role in ADPKD disease progression, modulating cyst epithelial apoptosis, proliferation, and interstitial inflammation (Ramalingam *et al*., 2020). For example, interstitial miR-214 attenuates inflammation and ADPKD progression (Lakhia *et al*., 2020). The miR-17 family is the primary therapeutic target for ADPKD via reducing cyst index, cyst proliferation, and kidney/body weight ratio (Yheskel *et al*., 2019). Patients with ADPKD may benefit from targeting miR-192 and -194 for the treatment of cyst formation and enlargement (Lee *et al*., 2019). miR-199a-5p dramatic upregulation in ADPKD rat model and ADPKD cell lines (Gu and Chan, 2012). miR-200 were reported to promote epithelial to interstitial transformation and Pkd1 to exert effects in the pathological progression of ADPKD (Patel *et al*., 2012). miRNAs may be useful therapeutic targets for ADPKD and may serve as significant diagnostic biomarkers in this disease.

Although there are growing bodies of studies describing the verification of the role of single miRNA expression in ADPKD, we still lack a systems-level understanding of miRNA-mRNA interaction network based on ADPKD patient samples. In ADPKD, miRNAs have a possible regulatory role, according to global miRNA and mRNA expression profiling. In the current study, the construction of a miRNA-mRNA network revealed novel molecular mechanisms through which ADPKD pathogenesis is promoted, which may support miRNA-based ADPKD diagnosis and treatment.

Therefore, in this study, the interactions between miRNA and mRNA were investigated by building a network between miRNAs and mRNAs in ADPKD utilizing GEO database. Several genes in the candidate miRNA-mRNA network may be useful for ADPKD diagnosis or as therapeutic targets (Supplementary Fig. S1).

MATERIALS AND METHODS

Datasets collection

The GEO database (https://www.ncbi.nlm.nih.gov/geoprofiles) was first used to search the data sets related to ADPKD by using the keywords "autosomal recessive polycystic kidney disease". Sample number n ≥3 was acquired and analyzed for each set of data. Only 4 results were obtained after searching. Next, GSE100812, GSE101811, GSE35831, and GSE7869 were downloaded. For miRNA expression profiling related to ADPKD, 3 renal cyst tissue samples of patients with ADPKD undergoing nephrectomy and 3 non-ADPKD renal tissue samples from patients undergoing surgery for clear cell renal cell carcinoma were obtained from GSE100812 (GPL18743 Agilent-021827 Human miRNA Microarray), while 10 serum samples of ADPKD and 10 serum samples from non-ADPKD were enrolled in GSE101811 (GPL23825 Exiqon microRNA Ready-to-Use PCR Human panel I+II). For gene/mRNA expression profiling in ADPKD, 2 renal cyst tissue samples of patients with ADPKD and 1 non-ADPKD renal tissue sample from patients undergoing surgery for clear cell renal cell carcinoma were obtained in GSE35831 (GPL6244 Affymetrix Human Gene 1.0 ST Array), while 18 renal cyst tissue samples of ADPKD and 3 normal renal cortical tissue were enrolled in GSE7869 (GPL570 Affymetrix Human Genome U133 Plus 2.0 Array).

Screening of differentially expressed miRNAs (DEMs) and differentially expressed genes (DEGs)

The expression data were normalized and pre-processed through the GEO2R (http://www.ncbi.nlm.nih.gov/geo/geo2r/) tool to perform DEMs and DEGs analysis between renal cyst tissue samples from ADPKD and normal renal cortical tissue samples from non-ADPKD. DEMs and DEGs were extracted by applying the inclusion criteria: Adjusted *P*-value (P <0.05) and $|\log_2 FC| \geq 0.5$. The miRNAs that overlapped in GSE100812 and GSE101811 were selected as DEMs. The overlapped mRNAs in GSE35831 and GSE7869 were selected as DEGs. A subsequent analysis was conducted using the DEMs and DEGs.

DEGs enrichment analysis

To predict the potential roles of DEGs, KEGG pathway and gene ontology (GO) (http://www.geneontology.org/) analyses were performed using Cluster Profiler R package (v3.0.0) (Yu *et al*., 2012; Fan *et al*., 2021). In GO analysis, GO terms contain three categories: biological process (BP), the cellular components (CC), and the molecular functions (MF) (Li *et al*., 2020). *P*-value of 0.05 was considered as the cutoff score. Gene set enrichment analysis (GSEA) was also performed using GSEA v4.1.0, with a threshold set at *P*-value <0.05 (Long *et al*., 2020).

Networks of miRNA-mRNA associated with transcription factors (TFs)

It is known that miRNA can bind to mRNA to

promote degradation. For these miRNA signatures, three databases including the miRDB (http://mirdb.org/miRDB/), miRTarBase (http://mirtarbase.mbc.nctu.edu.tw/), and TargetScan (http://www.targetscan.org/), were used and compared to identify the miRNAs' targets. On the basis of comparing predicted target genes with DEGs, the remaining overlapped genes and their interaction pairs were used to create miRNA-mRNA pairs.

With iRegulon software (http://apps.cytoscape.org/apps/iregulon), miRNA-mRNA networks were predicted. IRegulon can predict TFs that regulate gene sets. It calculates the motif enrichment analysis to predict the TFs. In order to analyze motif enrichment, multiple position weight matrices (PWM) are used. Finally, each motif is ranked and scored. TFs are predicted using the optimal motif. This network of miRNA-mRNA was then constructed for TFs.

Network analysis of miRNA-mRNA functional enrichment

The network of miRNAs and mRNAs was then investigated for potential biological processes and pathways. With the cluster profile R package, we analysed the GO functional enrichment (Jia *et al*., 2021). The miRNA-mRNA pathways that were enriched in KEGG pathways were subsequently identified using KEGG (http://www.genome.jp/kegg/) (Li *et al*., 2017). An enrichment analysis based on GO and KEGG pathway data was considered statistically significant when the *P*-value <0.05 was used (Xia *et al*., 2020).

Cell lines

The human ADPKD cell lines WT9-12 (CRL-2833) and normal renal HK-2 cells (CRL-2190) were obtained from the American Type Culture Collection (ATCC; Manassas, VA, USA). WT9-12 and HK-2 were cultured at 37°C with 5% CO_2 in Dulbecco's modified eagle's medium (DMEM/F12) containing 10% fetal bovine serum, 1% penicillin, and 1% streptomycin (Procell Life Science and Technology Co., Ltd., Wuhan, China).

Cell transfection

Overexpression of miRNA was achieved by transfection of miRNA mimic using the previously reported method (Lou *et al*., 2018). WT9-12 cells were plated on a six-well plates and propagated to 70~80% confluency. 20 nM scrambled miRNA (miRNA NC), miR-107, and miR-199a-3p miRNA mimics (RiboBio, Guangzhou, China) were transfected into cells using Lipofectamine 3000 (Invitrogen, Carlsbad, CA, USA) based on the manufacturer's instructions. After 48 h, cells were harvested for quantitative real-time polymerase chain reaction (qRT-PCR).

qRT-PCR

According to the procedure described previously (Fang *et al*., 2017), total RNA was extracted from HK-2 cells and WT9-12 cells and subjected to qRT-PCR. TRIzol reagent (CWBio, Beijing, China) and RNase-Free DNase kit was used to denature the RNA samples (Kirgen, Shanghai, China). The RNA was transcribed into cDNA using High-Capacity cDNA Reverse Transcription Kit (Qiagen, Mississauga, ON, Canada). miRNA reverse transcription primers and qRT-PCR primers obtained from Shanghai Sangon Biotech. Co. Ltd. (Shanghai, China) were shown in Table I. RT-qPCR was performed on the Light Cycler 480 Real-Time PCR System (Roche, Basel, Switzerland) and SYBR Green Master Mix (Toyobo, Osaka, Japan). qRT-PCR reaction program was: 95°C for 10 min, followed by 40 cycles of 95°C for 5 s, 55°C for 10 s, 72°C for 15 s, and 72°C for 7 s. Two copies of each qRT-PCR experiment were performed. The relative expression levels of miRNA and mRNA were normalized to the endogenous reference U6 small nuclear RNA and GAPDH, respectively, according to the $2^{-\Delta\Delta Ct}$ method.

Table I. qRT-PCR primer sequences.

Primer name	Primer sequence 5`→3`
GAPDH	F-CTGGGCTACACTGAGCACC
	R-AAGTGGTCGTTGAGGGCAATG
PRKCE	F-CAACGGACGCAAGATCGAG
	R-CTGGCTCCAGATCAATCCAGT
RUNX1T1	F-CTGAGACCTTTTGTCATCCCATT
	R-CCGTTTTCGTTCACATCGAGAA
SMARCE1	F-AGATTGGCAAGATTATTGGTGGC
	R-GCTTCTGCACGACTTTTTGCAT
CALU	F-AATAGACGCGGATAAAGATGGGT
	R-GCCATTGGTTTTCAACATTGTCA
FGF2	F-AGAAGAGCGACCCTCACATCA
	R-CGGTTAGCACACACTCCTTTG
TMED5	F-CTCGATAGCGACTTCACCTTTAC
	R-GGTGCTGAATGTATTGTCAAAGC
PNRC1	F-ACTTGCCACTAACCAAGATCAC
	R-TTGGAAGAACACTAGGAGAAGGT

Data analysis

Data are expressed as Mean ± standard error (SE). Differences were analyzed by using unpaired Student's t-test from GraphPad Prism version 6 (GraphPad Software, La Jolla, San Diego, CA, USA). *P*-values <0.05 were considered statistically significant.

RESULTS

Identification of DEMs and DEGs

DEMs between GSE100812 and GSE100811 were identified. GSE100812 contained 72 upregulated and 47 downregulated miRNAs, GSE100811 comprised 13 upregulated and 16 downregulated miRNAs. DEGs were identified from GSE35831 vs. GSE7869 comparison. 1263 genes were upregulated, and 903 genes were downregulated in GSE35831. While there are 6266 DEGs (3449 upregulated, 2817 downregulated) in GSE7869 (Supplementary Fig. S2). From these datasets, the 2 overlapped DEMs were identified of which 1 were upregulated and 1 were downregulated (Fig. 1a), while 1090 DEGs were screened (648 upregulated and 442 downregulated (Fig. 1b).

Analysis of DEGs for functional enrichment

As shown in Supplementary Figure S3 that the down-DEGs related to carbon metabolism and metabolic pathways, while the up-DEGs referred to pertussis and staphylococcus aureus infection. Furthermore, GO and KEGG enrichment analyses indicate that these DEGs mainly target inactivation of beta-alanine metabolism, alanine, aspartate, and glutamate metabolism in the kidney (Supplementary Fig. S3b and S3c).

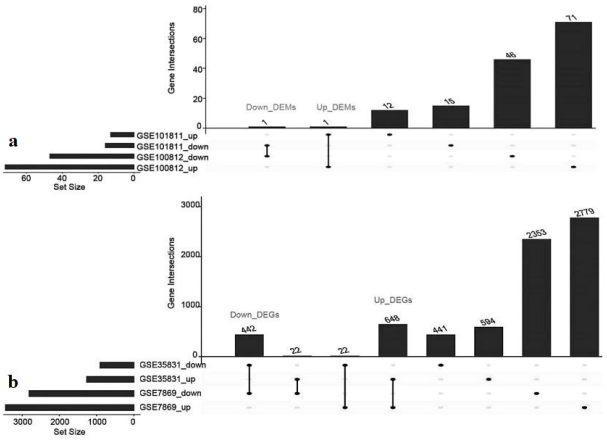

Fig. 1. DEMs and DEGs screening. a, DEMs screening (2 DEMs were screened, 1 up and 1 down). b, DEGs screening (1090 DEGs were screened).

Network of miRNAs and mRNAs

A miRNA-mRNA network is shown in Supplementary Figure S4, incorporating two miRNAs (miR-199a-3p, miR-107), seven mRNAs (FGF2, PNRC1, PRKCE, etc.) and top 10 transcription factors (for example, HOXA13 and EP-1G). In this miRNA network, hsa-miR-199a-3p was upregulated, while hsa-miR-107 was downregulated in ADPKD. Besides, RUNX1T1, SMARCE1, CALU, FGF2, and PNRC1 were upregulated, while PRKCE and TMED5 were downregulated in ADPKD (Fig. 2).

Analyzing the miRNA-mRNA network in terms of functional enrichment

These miRNA-mRNA networks were investigated by analyzing KEGG pathway enrichment and GO functional annotations from the KEGG database. GO consists of three categories: MF, BP, CC. In Supplementary Figure S5a and Supplementary Table SI, the top 30 enriched GO items are listed. Based on GO BP analysis, miRNA-mRNA networks are significantly enriched in the regulation of fibroblast migration, cell division, calcium entry, wound healing, and lipid metabolism. For CC analysis, miRNA-mRNA networks were significantly enriched in SWI/SNF complex, SWI/SNF superfamily type complex, npBAF complex, nBAF complex, ATPase complex, endoplasmic reticulum exit site, cis-Golgi network, sarcoplasmic reticulum, endoplasmic reticulum-Golgi intermediate compartment membrane, and sarcoplasm. KEGG enrichment analysis was performed for this miRNA-mRNA network. As listed in Table II and Supplementary Figure S5b, this miRNA-mRNA network was significantly enriched in acute myeloid leukemia, EGFR tyrosine kinase inhibitor resistance, Fc gamma R−mediated phagocytosis, melanoma, and Type II diabetes mellitus.

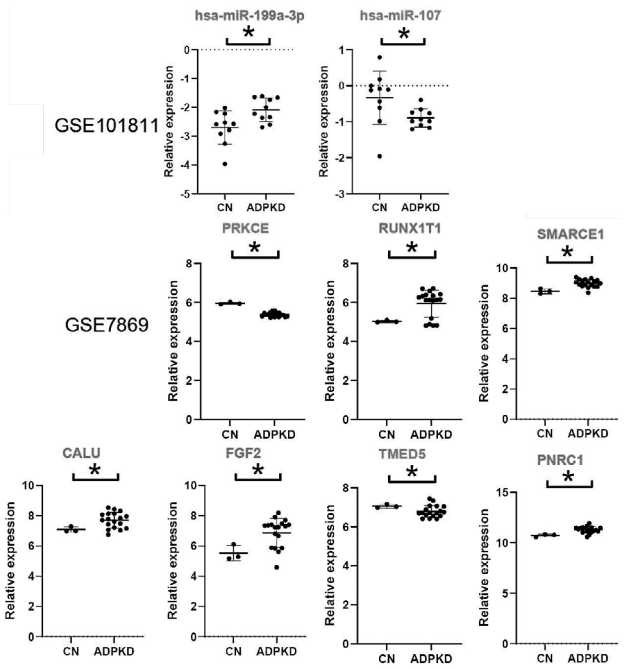

Fig. 2. miRNA-mRNA network expression in ADPKD.

Table II. The KEGG pathways of DEMs in the DEMs-DEGs regulatory network.

Description	Count	P value	Gene ID
Type II diabetes mellitus	1	0.022	hsa04930
Acute myeloid leukemia	1	0.033	hsa05221
Melanoma	1	0.035	hsa05218
EGFR tyrosine kinase inhibitor resistance	1	0.038	hsa01521
Fc gamma R-mediated phagocytosis	1	0.047	hsa04666
Inflammatory mediator regulation of TRP channels	1	0.047	hsa04750
Aldosterone synthesis and secretion	1	0.047	hsa04925
AGE-RAGE signaling pathway in diabetic complications	1	0.048	hsa04933

Identification of several potential miRNAs and their target gene expression in vitro

To confirm the results of the mRNA expression in Figure 2, qRT-PCR for target mRNAs was performed in WT9-12 cells and HK-2 cells. As shown in Figure 3, comparing ADPKD cells to normal cells, PRKCE (Fig. 3a), TEMED5 (Fig. 3f) were significantly downregulated whereas RUNX1T1 (Fig. 3b), CALU (Fig. 3d), and FGF2 (Fig. 3e) were markedly up-regulated. In ADPKD cells, however, no significant increase in SMARCE1 (Fig. 3c) or PNRC1 (Fig. 3g) expression was observed.

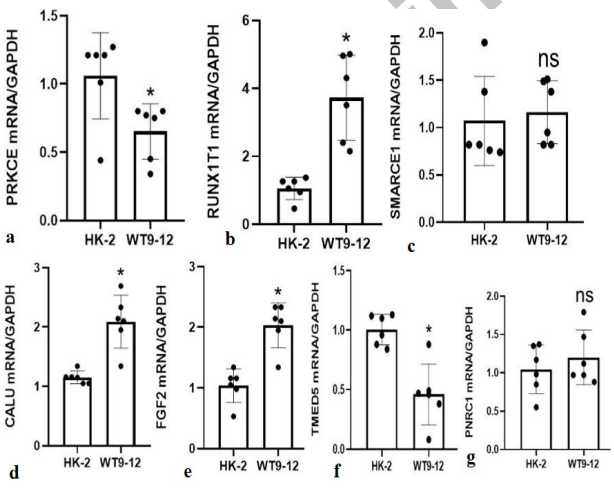

Fig. 3. qRT-PCR validation of target mRNA expression in HK-2 and WT9-12 cells. a, PRKCE; b, RUNX1T1; c, SMARCE1; d, CALU; e, FGF2; f, TMED5; g, PNRC1.
Notes: n = 6 per group; **P* <0.05 vs. HK-2. Data are Mean ± SE, results were obtained after repeating the experiment three times.

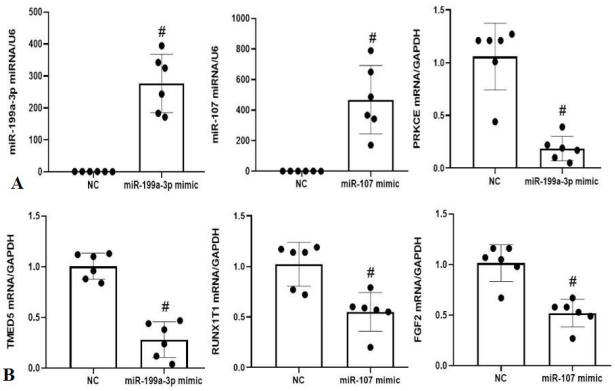

Fig. 4. The expression levels of target genes (A and B) and (C-F) the alteration of target gene after transfection in WT9-12.
a, miR-199a-3p miRNA; b, miR-107 miRNA; c, PRKCE; d, TMED5; e, RUNX1T1; f, FGF2.
Notes: n= 6 per group. # *P* <0.05 vs. NC. Data are Mean ± SE. Similar results were obtained after repeating the experiment three times.

Compared to miRNA NC transfected in WT9-12 cells, miRNA-199a-3p (Fig. 4a) and miR-107 (Fig. 4b) miRNA levels were significantly increased compared to miRNA NC transfected in the same cells. The expression of PRKCE and TMED5 was attenuated by miR-199a-3p overexpression in Figure 4c and 4d, respectively. Overexpression of miR-107 attenuated RUNX1T1 (Fig. 4e) and FGF2 (Fig. 4f) expression. Together, these data strongly suggested that miR-199a-3p and miR-107 had an important pathophysiological role in the development of ADPKD.

DISCUSSION

ADPKD is a fairly common hereditary renal disease, and there is no radical treatment and imposes substantial societal costs (Cloutier *et al*., 2020). The regulatory mechanisms underlying miRNA functions in ADPKD have previously been studied (Li and Sun, 2020). Using GEO database data, we analyzed a differential expression analysis of miRNA and mRNA.

miRNA participates in regulating PKD1, PKD2, and other genes that involved in ADPKD pathogenesis (Tan *et al*., 2011). The dysregulation of miRNA is relevant to pathologic mechanisms of cyst formation as potential biomarker and innovative therapies in ADPKD (Yheskel and Patel, 2017). Over the past few years, numerous studies revealed that alteration of miRNAs and their downstream target gene expression levels is closely associated with ADPKD progression (Hajarnis *et al*., 2015;

Li and Sun, 2020; Ramalingam *et al*., 2020). ADPKD and normal kidney showed differential expression of DEMs and DEGs in our study. Utilizing combined DEGs, we further analyzed GO and KEGG pathways for identifying biological functions. In GO biological processes, certain genes were found to be concentrated in several process areas, including migration of fibroblasts and epithelial cells, calcium signaling, and cell division.

It is believed that miRNAs function by degrading or inhibiting specific mRNAs in the body (Zhi *et al*., 2019). A total of 1090 DEGs (648 upregulated and 442 downregulated) and 2 DEMs (1 upregulated and 1 downregulated) were found between ADPKD and non-ADPKD patients. hsa-miR-199a-3p unregulated DEMs and hsa-miR-107 downregulated DEMs were finally identified. The results of *in silico* analyses were further supported by subsequent experiments. qRT-PCR validation identified that RUNX1T1, CALU, and FGF2 mRNA expression levels were significantly upregulated but PRKCE, TMED5 mRNA expression levels were markedly downregulated in WT9-12 compared with HK-2 cells. In addition, we confirmed that overexpression of miR-199-3p mimics inhibited PRKCE and TMED5 expression. Meanwhile, miR-107 mimic overexpression could downregulated the mRNA expression level of RUNX1T1, FGF2. Experimental results indicate that miR-199a-3p-TMED5, miR-107-FGF2, miR-107-RUNX1T1 and miR-199a-3p-PRKCE are the most beneficial miRNA-mRNA regulatory pathways among all identified miRNA-mRNA pathways. The importance of these regulatory pathways needs to be emphasized in the future.

Several cancer tissues show downregulation of hsa-miR-199a-3p, which is related to tumor malignancy grades, such as metastasis, invasion, and proliferation (Shin and Chu, 2014). The inactivation of the IKKβ/NF-κB pathway by miR-199a-3p protects HK-2 cells from high glucose induced damage; demonstrating miR-199a-3p could be used for the treatment of diabetic nephropathy (Zhang *et al*., 2020b). Esophageal cancer cells are less likely to multiply when miR-199a-3p targets p21, activating kinase 4 in the process (Phatak *et al*., 2018). Further findings showed that miR-199a-3p inhibits the colonization, invasion, proliferation, and migration of clear cell renal cell carcinoma cells (Liu *et al*., 2018). According to Tao *et al*. (2019), MiR-199a-3p inhibits CD151 expression in cardiomyocytes. Human diseases can therefore be treated by targeting miR-199a-3p, though the exact mechanism varies with the type of cell. MiR-199a-3p overexpression suppressed PRKCE and TMED5 in ADPKD cells, suggesting that it inhibits the pathogenic effects of ADPKD. Due to the complex regulatory functions of miR-199a-3p, its mechanism of action in ADPKD remains to be studied in depth. The pathogenesis of renal disease is also attributed to miR-107 (Jiang and Zhou, 2014). Suppressing miR-107 in endothelial cells prevents renal tubular damage in septic acute kidney injury (Wang *et al*., 2017). There is a marked decline in miR-107 levels even in patients who have the earliest stages of the disease. A study by our group showed that ADPKD cells overexpressed miR-107 showed a decreased production of RUNX1T1 and FGF2. Combined, these findings support our hypothesis that miR-199a-3p and miR-107 contribute to ADPKD progression.

Of note, we found upregulation (e.g., FGF2 and RUNX1T1) and downregulation (TMED5 and PRKCE) of multiple developmental genes, and transcription factors (TFs) (e.g., BBX, VDR, TCF12, and EP300). Most of these genes have been identified as key regulators in ADPKD. FGF2, for instance, belongs to the fibroblast growth factor family, which regulates migration, differentiation, and cell growth (Nawrocka *et al*., 2020). Basic fibroblast growth factor increases with the progression of kidney cystic lesions in DBA/2FG-pcy mice (Nakamura *et al*., 1993). Both unilateral ureteral obstruction mice and diabetic mice were all exhibited significantly renal fibrosis, concomitant with a marked FGF2 production (Dong *et al*., 2020; Guan *et al*., 2014). Our data also revealed that ADPKD cells were significantly upregulated compared with HK-2 cells in terms of FGF2. An ETO family member, RUNX1T1, is conservative in ideology (Swart and Heidenreich, 2021). Initially, RUNX1T1 was identified as a possible component of acute myeloid leukemia translocations, and BMP4 and TGF-β2 have been shown to mediate the angiogenic activity of RUNX1T1 (Liao *et al*., 2017). RUNX1T1 will improve the therapeutic effect of ischemia by promoting the formation of new blood vessels (Liao *et al*., 2017). TMED5, located in region 1p21-22 of chromosome, is related to the pathogenesis of myeloma and bladder cancer (Scaravilli *et al*., 2014). TMED5 overexpression induces malignant phenotypes such as cell migration, proliferation, and apoptosis (Zou *et al*., 2021). Based on our results, miR-199a-3p may directly target and inhibit TMED5. Tumor aggressiveness is linked to PRKCE. It has been suggested that because it is elevated in a variety of malignancies, it plays a role in malignant transformation and metastasis (Zhang *et al*., 2020a). It has been reported that PRKCE modulates tumorigenesis and drug resistance by targeting several miRNAs (Korner *et al*., 2013). In the current study, we speculate that PRKCE gene can also be regulated by miR-199a-3p miRNA in ADPKD cells. It has been demonstrated that TFs are capable of regulating miRNA expression in the past. For example, VDR expression is the association with kidney volume in ADPKD patients (Vendramini *et al*., 2019). In the future, more experiments

on the role of these predicted TFs in ADPKD are needed.

The following limitations of the current study need to be taken into account: (1) The underlying mechanisms of ADPKD have not been fully explored, although several mRNA and miRNA markers have been linked to the disease. (2) It is essential to provide more experimental evidence to support the bioinformatics analysis results that were derived from qRT-PCR validation. (3) The following comprehensive analysis requires more clinical information.

CONCLUSIONS

FGF2, TMED5, RUNX1T1, and PRKCE mRNA expression were identified as potential ADPKD biomarkers. Prognostic markers such as miR-107 and miR-199a-3p may also help clinicians decide how to treat ADPKD. This study shows that the miRNA-mRNA regulatory axis has a relatively comprehensive potential mechanism in the pathogenesis of ADPKD. As a future treatment for ADPKD, it may target the established miRNA-mRNA regulatory network to improve prognosis.

Funding

This research was funded by the National Natural Science Foundation of China (No. 82000400), the Weifang Science and Technology Development Plan (No. 2021YX043) and the Provincial Undergraduate Training Programs for Innovation and Entrepreneurship (No. S202210438060).

Ethical statement

There are no studies conducted on animals or humans.

Supplementary material

There is supplementary material associated with this article. Access the material online at: https://dx.doi.org/10.17582/journal.pjz/20210728090730

Statement of conflict of interest

The authors have declared no conflict of interest.

REFERENCES

Bai, Y.P., Zhang, J.X., Sun, Q., Zhou, J.P., Luo, J.M., He, L.F., Lin, X.C., Zhu, L.P., Wu, W.Z., Wang, Z.Y. and Zhang, G.G., 2018. Induction of microRNA-199 by nitric oxide in endothelial cells is required for nitrovasodilator resistance via targeting of prostaglandin I2 synthase. *Circulation,* **138**: 397-411. https://doi.org/10.1161/CIRCULATIONAHA.117.029206

Cloutier, M., Manceur, A.M., Guerin, A., Aigbogun, M.S., Oberdhan, D. and Gauthier-Loiselle, M., 2020. The societal economic burden of autosomal dominant polycystic kidney disease in the United States. *BMC Hlth. Serv. Res.*, **20**: 126. https://doi.org/10.1186/s12913-020-4974-4

Cornec-Le-Gall, E., Alam, A. and Perrone, R.D., 2019. Autosomal dominant polycystic kidney disease. *Lancet*, **393**: 919-935. https://doi.org/10.1016/S0140-6736(18)32782-X

Dong, Q.L., Zhao, X.H., Wang, Q., Zhang, L.P., Yan, X.H., Wang, X.M., Li, Z.J. and Sun, Y., 2020. Anti-aging gene Klotho ameliorates diabetic nephropathy in mice by inhibiting FGF2 signaling pathway. *J. Biol. Regul. Homeost. Agents*, **34**: 1369-1377.

Fan, S.G., Guo, Y.H. and Xu, Y.H., 2021. Comparative transcriptome analysis of the ovary and testis in noble scallop (*Chlamys nobilis*). *Pakistan J. Zool.*, **53**: 251-261. https://doi.org/10.17582/journal.pjz/20190125080146

Fang, H., Xu, C., Lu, A., Zou, C.J., Xie, S., Chen, Y., Zhou, L., Liu, M., Wang, L., Wang, W. and Yang, T., 2017. (Pro) renin receptor mediates albumin-induced cellular responses: Role of site-1 protease-derived soluble (pro)renin receptor in renal epithelial cells. *Am. J. Physiol. Cell Physiol.*, **313**: C632-C643. https://doi.org/10.1152/ajpcell.00006.2017

Gevers, T.J. and Drenth, J.P., 2011. Somatostatin analogues for treatment of polycystic liver disease. *Curr. Opin. Gastroenterol.*, **27**: 294-300. https://doi.org/10.1097/MOG.0b013e328343433f

Gu, S. and Chan, W.Y., 2012. Flexible and versatile as a chameleon-sophisticated functions of microRNA-199a. *Int. J. mol. Sci.*, **13**: 8449-8466. https://doi.org/10.3390/ijms13078449

Guan, X., Nie, L., He, T., Yang, K., Xiao, T., Wang, S., Huang, Y., Zhang, J., Wang, J., Sharma, K., Liu, Y. and Zhao, J., 2014. Klotho suppresses renal tubulo-interstitial fibrosis by controlling basic fibroblast growth factor-2 signalling. *J. Pathol.*, **234**: 560-572. https://doi.org/10.1002/path.4420

Hajarnis, S., Lakhia, R. and Patel, V., 2015. *MicroRNAs and polycystic kidney disease*. Exon Publications. pp. 313-334. https://doi.org/10.15586/codon.pkd.2015.ch13

Idowu, J., Home, T., Patel, N., Magenheimer, B., Tran, P.V., Maser, R.L., Ward, C.J., Calvet, J.P., Wallace, D.P. and Sharma, M., 2018. Aberrant regulation of Notch3 signaling pathway in polycystic kidney disease. *Sci. Rep.*, **8**: 3340. https://doi.org/10.1038/

s41598-018-21132-3

Jia, N.Y., Liu, X.Z., Zhang, Z. and Zhang, H., 2021. Weighted gene co-expression network analysis reveals different immunity but shared renal pathology between IgA nephropathy and lupus nephritis. *Front. Genet.*, **12**: 634171. https://doi.org/10.3389/fgene.2021.634171

Jiang, Z.P. and Zhou, T.B., 2014. Role of miR-107 and its signaling pathways in diseases. *J. Recept. Signal Transduct.*, **34**: 338-341. https://doi.org/10.3109/10799893.2014.896383

Korner, C., Keklikoglou, I., Bender, C., Worner, A., Munstermann, E. and Wiemann, S., 2013. MicroRNA-31 sensitizes human breast cells to apoptosis by direct targeting of protein kinase C epsilon (PKCepsilon). *J. biol. Chem.*, **288**: 8750-8761. https://doi.org/10.1074/jbc.M112.414128

Kotani, A., Ha, D., Hsieh, J., Rao, P.K., Schotte, D., den Boer, M.L., Armstrong, S.A. and Lodish, H.F., 2009. miR-128b is a potent glucocorticoid sensitizer in MLL-AF4 acute lymphocytic leukemia cells and exerts cooperative effects with miR-221. *Blood,* **114**: 4169-4178. https://doi.org/10.1182/blood-2008-12-191619

Lakhia, R., 2020. The role of PPARalpha in autosomal dominant polycystic kidney disease. *Curr. Opin. Nephrol. Hypertens.,* **29**: 432-438. https://doi.org/10.1097/MNH.0000000000000615

Lakhia, R., Yheskel, M., Flaten, A., Quittner-Strom, E.B., Holland, W.L. and Patel, V., 2018. PPARalpha agonist fenofibrate enhances fatty acid beta-oxidation and attenuates polycystic kidney and liver disease in mice. *Am. J. Physiol. Renal Physiol.,* **314**: 453. https://doi.org/10.1152/ajprenal.00352.2017

Lakhia, R., Yheskel, M., Flaten, A., Ramalingam, H., Aboudehen, K., Ferre, S., Biggers, L., Mishra, A., Chaney, C., Wallace, D.P., Carroll, T., Igarashi, P. and Patel, V., 2020. Interstitial microRNA miR-214 attenuates inflammation and polycystic kidney disease progression. *JCI Insight*, **5**: e133785. https://doi.org/10.1172/jci.insight.133785

Lee, E.C., Valencia, T., Allerson, C., Schairer, A., Flaten, A., Yheskel, M., Kersjes, K., Li, J., Gatto, S., Takhar, M., Lockton, S., Pavlicek, A., Kim, M., Chu, T., Soriano, R., Davis, S., Androsavich, J.R., Sarwary, S., Owen, T., Kaplan, J., Liu, K., Jang, G., Neben, S., Bentley, P., Wright, T. and Patel, V., 2019. Discovery and preclinical evaluation of anti-miR-17 oligonucleotide RGLS4326 for the treatment of polycystic kidney disease. *Nat. Commun.,* **10**: 4148. https://doi.org/10.1038/s41467-019-11918-y

Li, D. and Sun, L., 2020. MicroRNAs and polycystic kidney disease. *Kidney Med.*, **2**: 762-770. https://doi.org/10.1016/j.xkme.2020.06.013

Li, Y., Jin, L., Dong, A., Zhou, X. and Yuan, H., 2017. Microarray expression profile analysis of long non-coding RNAs in optineurin E50K mutant transgenic mice. *Mol. Med. Rep.*, **16**: 1255-1261. https://doi.org/10.3892/mmr.2017.6722

Li, Y., Wang, Q., Ning, N., Tang, F.L. and Wang, Y., 2020. Bioinformatic analysis reveals *MIR502* as a potential tumour suppressor in ovarian cancer. *J. Ovarian Res.*, **13**: 1-16. https://doi.org/10.1186/s13048-020-00683-y

Liao, K.H., Chang, S.J., Chang, H.C., Chien, C.L., Huang, T.S., Feng, T.C., Lin, W.W., Shih, C.C., Yang, M.H., Yang, S.H., Lin, C.H., Hwang, W.L. and Lee, O.K., 2017. Endothelial angiogenesis is directed by RUNX1T1-regulated VEGFA, BMP4 and TGF-beta2 expression. *PLoS One*, **12**: e0179758. https://doi.org/10.1371/journal.pone.0179758

Liu, J., Liu, B., Guo, Y., Chen, Z., Sun, W., Gao, W., Wu, H. and Wang, Y., 2018. MiR-199a-3p acts as a tumor suppressor in clear cell renal cell carcinoma. *Pathol. Res. Pract.*, **214**: 806-813. https://doi.org/10.1016/j.prp.2018.05.005

Long, Y., Li, X., Li, F., Ge, G., Liu, R., Song, G., Li, Q., Qiao, Z. and Cui, Z., 2020. Transcriptional programs underlying cold acclimation of common carp (*Cyprinus carpio* L.). *Front. Genet.*, **11**: 556418. https://doi.org/10.3389/fgene.2020.556418

Lou, W., Chen, J., Ding, B., Chen, D., Zheng, H., Jiang, D., Xu, L., Bao, C., Cao, G. and Fan, W., 2018. Identification of invasion-metastasis-associated microRNAs in hepatocellular carcinoma based on bioinformatic analysis and experimental validation. *J. Transl. Med.,* **16**: 266. https://doi.org/10.1186/s12967-018-1639-8

Nakamura, T., Ebihara, I., Nagaoka, I., Tomino, Y., Nagao, S., Takahashi, H. and Koide, H., 1993. Growth factor gene expression in kidney of murine polycystic kidney disease. *J. Am. Soc. Nephrol.,* **3**: 1378-1386. https://doi.org/10.1681/ASN.V371378

Nawrocka, D., Krzyscik, M.A., Opalinski, L., Zakrzewska, M. and Otlewski, J., 2020. Stable fibroblast growth factor 2 dimers with high pro-survival and mitogenic potential. *Int. J. mol. Sci.,* **21**: 4108. https://doi.org/10.3390/ijms21114108

Nobakht, N., Hanna, R.M., Al-Baghdadi, M., Ameen, K.M., Arman, F., Nobahkt, E., Kamgar, M. and Rastogi, A., 2020. Advances in autosomal dominant

polycystic kidney disease: A clinical review. *Kidney Med.*, **2**: 196-208. https://doi.org/10.1016/j.xkme.2019.11.009

Patel, V., Hajarnis, S., Williams, D., Hunter, R., Huynh, D. and Igarashi, P., 2012. MicroRNAs regulate renal tubule maturation through modulation of Pkd1. *J. Am. Soc. Nephrol.*, **23**: 1941-1948. https://doi.org/10.1681/ASN.2012030321

Phatak, P., Burrows, W.M., Chesnick, I.E., Tulapurkar, M.E., Rao, J.N., Turner, D.J., Hamburger, A.W., Wang, J.Y. and Donahue, J.M., 2018. MiR-199a-3p decreases esophageal cancer cell proliferation by targeting p21 activated kinase 4. *Oncotarget*, **9**: 28391-28407. https://doi.org/10.18632/oncotarget.25375

Radadiya, P.S., Thornton, M.M., Daniel, E.A., Idowu, J.Y., Wang, W., Magenheimer, B., Subramaniam, D., Tran, P.V., Calvet, J.P., Wallace, D.P. and Sharma, M., 2021. Quinomycin A reduces cyst progression in polycystic kidney disease. *FASEB J.*, **35**: e21533. https://doi.org/10.1096/fj.202002490R

Ramalingam, H., Yheskel, M. and Patel, V., 2020. Modulation of polycystic kidney disease by non-coding RNAs. *Cell. Signal.*, **71**: 109548. https://doi.org/10.1016/j.cellsig.2020.109548

Scaravilli, M., Asero, P., Tammela, T.L., Visakorpi, T. and Saramaki, O.R., 2014. Mapping of the chromosomal amplification 1p21-22 in bladder cancer. *BMC Res. Notes,* **7**: 547. https://doi.org/10.1186/1756-0500-7-547

Shen, A.W., Fu, L.L., Lin, L., Sun, B., Song, D.X., Wang, W.T., Wang, Y.H., Yin, P.R. and Yu, S.Q., 2020. SNX9 inhibits cell proliferation and cyst development in autosomal dominant polycystic kidney disease via activation of the hippo-YAP signaling pathway. *Front. Cell Dev. Biol.*, **8**: 811. https://doi.org/10.3389/fcell.2020.00811

Shi, M.Y., Yan, X.L., Han, P.P., Tang Y.J. and Li, H.X., 2020. Microarray and bioinformatics analysis of differentially-expressed MicroRNAs in Wnt/B-Catenin signaling-activated bovine skeletal muscle satellite cells. *Pakistan J. Zool.*, **52**: 2071-2080. https://doi.org/10.17582/journal.pjz/20190108100153

Shin, V.Y. and Chu, K.M., 2014. MiRNA as potential biomarkers and therapeutic targets for gastric cancer. *World J. Gastroenterol.*, **20**: 10432-10439. https://doi.org/10.3748/wjg.v20.i30.10432

Song, A., Zhang, C. and Meng, X., 2021. Mechanism and application of metformin in kidney diseases: An update. *Biomed. Pharmacother.*, **138**: 111454. https://doi.org/10.1016/j.biopha.2021.111454

Swart, L.E. and Heidenreich, O., 2021. The RUNX1/RUNX1T1 network: Translating insights into therapeutic options. *Exp. Hematol.*, **94**: 1-10. https://doi.org/10.1016/j.exphem.2020.11.005

Tan, Y.C., Blumenfeld, J. and Rennert, H., 2011. Autosomal dominant polycystic kidney disease: Genetics, mutations and microRNAs. *Biochim. biophys. Acta, Mol. Basis Dis.,* **1812**: 1202-1212. https://doi.org/10.1016/j.bbadis.2011.03.002

Tao, Y., Zhang, H., Huang, S., Pei, L., Feng, M., Zhao, X., Ouyang, Z., Yao, S., Jiang, R. and Wei, K., 2019. miR-199a-3p promotes cardiomyocyte proliferation by inhibiting Cd151 expression. *Biochem. biophys. Res. Commun.,* **516**: 28-36. https://doi.org/10.1016/j.bbrc.2019.05.174

Vendramini, L.C., Dalboni, M.A., de Carvalho Jr, J.T.G., Batista, M.C., Nishiura, J.L. and Heilberg, I.P., 2019. Association of vitamin D levels with kidney volume in autosomal dominant polycystic kidney disease (ADPKD). *Front. Med.*, **6**: 112. https://doi.org/10.3389/fmed.2019.00112

Wang, S., Zhang, Z., Wang, J. and Miao, H., 2017. MiR-107 induces TNF-alpha secretion in endothelial cells causing tubular cell injury in patients with septic acute kidney injury. *Biochem. biophys. Res. Commun.,* **483**: 45-51. https://doi.org/10.1016/j.bbrc.2017.01.013

Xia, Q., Liu, M., Li, H., Tian, L., Qi, J. and Zhang, Y., 2020. Network pharmacology strategy to investigate the pharmacological mechanism of HuangQiXiXin decoction on cough variant asthma and evidence-based medicine approach validation. *Evid. Based Complement. Altern. Med.*, **2020**: 3829092. https://doi.org/10.1155/2020/3829092

Xu, Y., Li, A., Wu, G. and Liang, C., 2017. Perspectives of gene therapies in autosomal dominant polycystic kidney disease. *Curr. Gene Ther.*, **17**: 43-49. https://doi.org/10.2174/1566523217666170510152808

Xue, C. and Mei, C.L., 2019. Polycystic kidney disease and renal fibrosis. *Adv. exp. Med. Biol.*, **1165**: 81-100. https://doi.org/10.1007/978-981-13-8871-2_5

Yheskel, M. and Patel, V., 2017. Therapeutic microRNAs in polycystic kidney disease. *Curr. Opin. Nephrol. Hypertens.*, **26**: 282-289. https://doi.org/10.1097/MNH.0000000000000333

Yheskel, M., Lakhia, R., Cobo-Stark, P., Flaten, A. and Patel, V., 2019. Anti-microRNA screen uncovers miR-17 family within miR-17~92 cluster as the primary driver of kidney cyst growth. *Sci. Rep.*, **9**: 1920. https://doi.org/10.1038/s41598-019-38566-y

Yu, G., Wang, L.G., Han, Y. and He, Q.Y., 2012. clusterProfiler: an R package for comparing

biological themes among gene clusters. *OMICS: J. Integr. Biol.*, **16**: 284-287. https://doi.org/10.1089/omi.2011.0118

Zhang, G.F., Wu, J.C., Wang, H.Y., Jiang, W.D. and Qiu, L., 2020a. Overexpression of microRNA-205-5p exerts suppressive effects on stem cell drug resistance in gallbladder cancer by down-regulating PRKCE. *Biosci. Rep.,* **40**: BSR20194509. https://doi.org/10.1042/BSR20194509

Zhang, R., Qin, L. and Shi, J., 2020b. MicroRNA199a3p suppresses high glucoseinduced apoptosis and inflammation by regulating the IKKbeta/NFkappaB signaling pathway in renal tubular epithelial cells. *Int. J. mol. Med.*, **46**: 2161-2171. https://doi.org/10.3892/ijmm.2020.4751

Zhi, Y., Xu, C., Sui, D., Du, J., Xu, F.J. and Li, Y., 2019. Effective delivery of hypertrophic miRNA inhibitor by cholesterol-containing nanocarriers for preventing pressure overload induced cardiac hypertrophy. *Adv. Sci.,* **6**: 1900023. https://doi.org/10.1002/advs.201900023

Zou, H., Chen, H., Liu, S. and Gan, X., 2021. Identification of a novel circ_0018289/miR-183-5p/TMED5 regulatory network in cervical cancer development. *World J. Surg. Oncol.,* **19**: 246. https://doi.org/10.1186/s12957-021-02350-y

Pakistan J. Zool., pp 1-10, 2022. **DOI**: https://dx.doi.org/10.17582/journal.pjz/20210728090730

Supplementary Material

Identification of ADPKD-Related Key miRNAs by Constructing a miRNA-mRNA Interaction Network and Experimental Verification

Hui Fang*, Kai Xue and Teng Yang

School of Pharmacy, Weifang Medical University, Weifang 261053, Shandong, China.

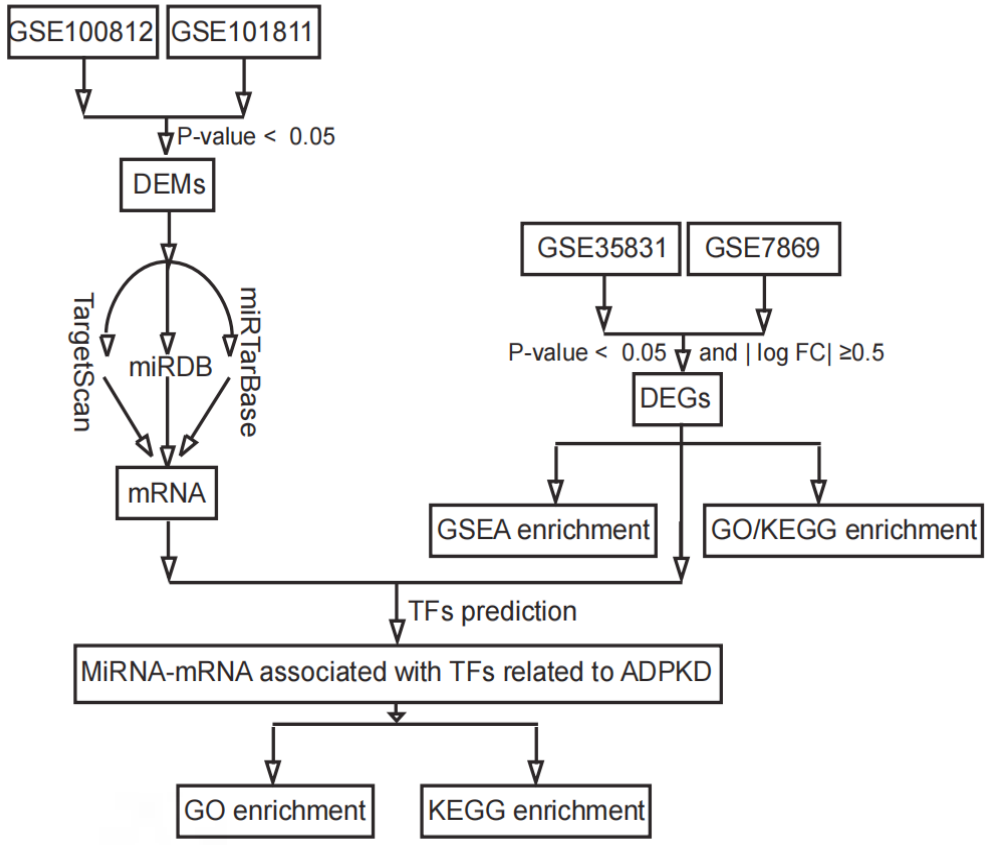

Supplementary Fig. S1. An overview of the bioinformatics workflow in this study.

* Corresponding author: fanghui8@wfmc.edu.cn
0030-9923/2022/0001-0001 $ 9.00/0

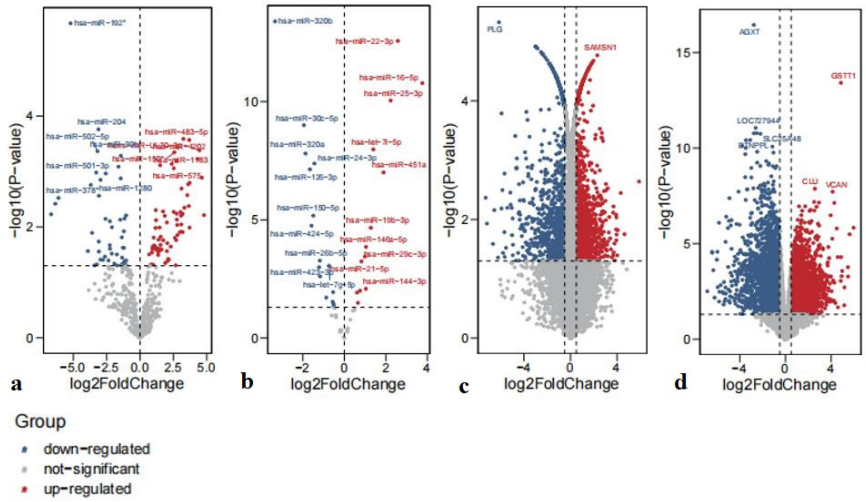

Supplementary Fig. S2. Volplot of DEMs and DEGs. a, miRNA (GSE100812); b, miRNA (GSE100811); c, mRNA (GSE35831); d, mRNA (GSE7869).

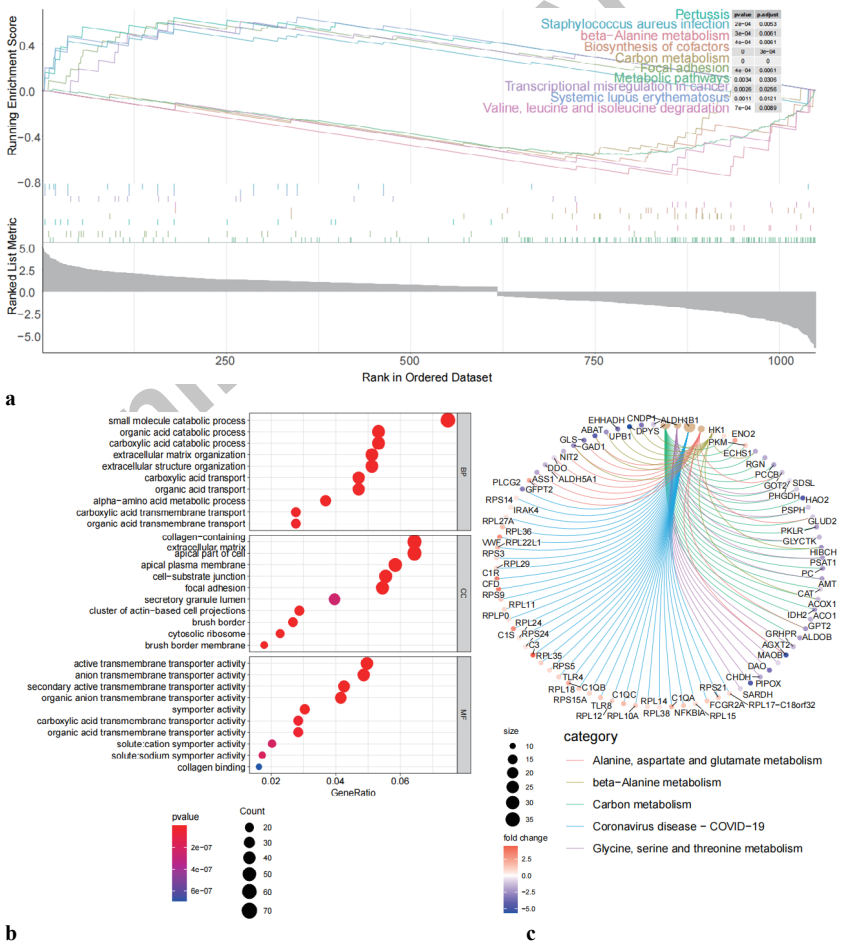

Supplementary Fig. S3. Functional enrichment analysis of DEGs. a, GSEA analysis. b, GO analysis of DEGs. c, KEGG analysis of DEGs.

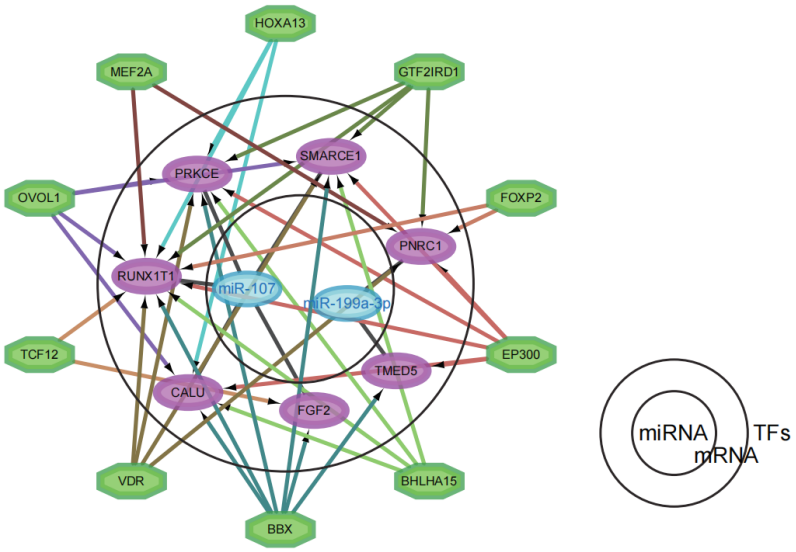

Supplementary Fig. S4. miRNA-mRNA network associated with TFs

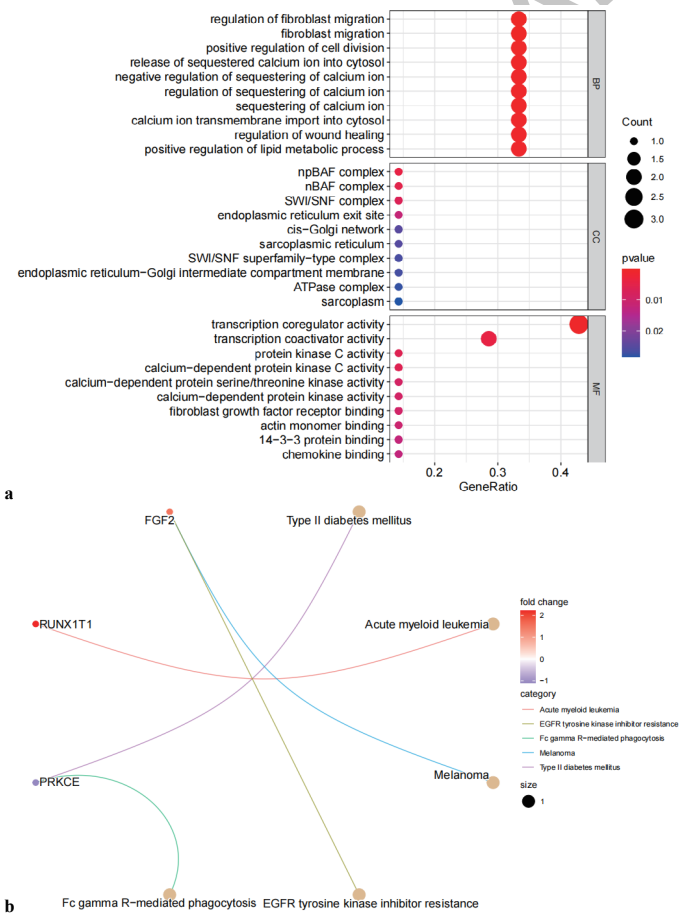

Supplementary Fig. S5. Functional enrichment analysis of miRNA-mRNA network. a, GO analysis of miRNA-mRNA network. b, KEGG analysis of miRNA-mRNA network.

Supplementary Table SI. GO analysis of miRNA network.

Description	P value	Gene	Count
regulation of fibroblast migration	0.000	PRKCE/FGF2	2
fibroblast migration	0.000	PRKCE/FGF2	2
positive regulation of cell division	0.000	PRKCE/FGF2	2
release of sequestered calcium ion into cytosol	0.001	PRKCE/FGF2	2
negative regulation of sequestering of calcium ion	0.001	PRKCE/FGF2	2
regulation of sequestering of calcium ion	0.001	PRKCE/FGF2	2
sequestering of calcium ion	0.001	PRKCE/FGF2	2
calcium ion transmembrane import into cytosol	0.001	PRKCE/FGF2	2
regulation of wound healing	0.001	PRKCE/FGF2	2
positive regulation of lipid metabolic process	0.001	PRKCE/FGF2	2
calcium ion transport into cytosol	0.001	PRKCE/FGF2	2
regulation of cell division	0.001	PRKCE/FGF2	2
positive regulation of epithelial cell migration	0.001	PRKCE/FGF2	2
cytosolic calcium ion transport	0.001	PRKCE/FGF2	2
regulation of response to wounding	0.001	PRKCE/FGF2	2
maintenance of location in cell	0.002	PRKCE/FGF2	2
endothelial cell chemotaxis to fibroblast growth factor	0.003	FGF2	1
mucus secretion	0.003	PRKCE	1
regulation of endothelial cell chemotaxis to fibroblast growth factor	0.003	FGF2	1
regulation of epithelial cell migration	0.004	PRKCE/FGF2	2
cell chemotaxis to fibroblast growth factor	0.004	FGF2	1
regulation of cell chemotaxis to fibroblast growth factor	0.004	FGF2	1
negative regulation of sodium ion transmembrane transporter activity	0.004	PRKCE	1
calcium ion transmembrane transport	0.004	PRKCE/FGF2	2
regulation of skeletal muscle satellite cell proliferation	0.004	FGF2	1
positive regulation of synaptic transmission, GABAergic	0.004	PRKCE	1
locomotory exploration behavior	0.004	PRKCE	1
negative regulation of sodium ion transmembrane transport	0.004	PRKCE	1
positive regulation of cytosolic calcium ion concentration	0.004	PRKCE/FGF2	2
maintenance of location	0.004	PRKCE/FGF2	2
skeletal muscle satellite cell proliferation	0.004	FGF2	1
regulation of skeletal muscle cell proliferation	0.004	FGF2	1
regulation of cell fate specification	0.004	FGF2	1
cellular response to ethanol	0.004	PRKCE	1
Golgi ribbon formation	0.004	TMED5	1
macrophage activation involved in immune response	0.005	PRKCE	1
positive regulation of cell fate commitment	0.005	FGF2	1
positive regulation of fibroblast migration	0.005	PRKCE	1
skeletal muscle cell proliferation	0.005	FGF2	1
positive regulation of endothelial cell chemotaxis	0.005	FGF2	1

Table continued on next page.....

Description	P value	Gene	Count
hyaluronan catabolic process	0.005	FGF2	1
cellular response to prostaglandin E stimulus	0.005	PRKCE	1
regulation of cytosolic calcium ion concentration	0.005	PRKCE/FGF2	2
epithelial cell migration	0.005	PRKCE/FGF2	2
epithelium migration	0.005	PRKCE/FGF2	2
tissue migration	0.006	PRKCE/FGF2	2
nucleosome disassembly	0.006	SMARCE1	1
negative regulation of sodium ion transport	0.006	PRKCE	1
cellular glucuronidation	0.006	PRKCE	1
chromatin disassembly	0.006	SMARCE1	1
protein-DNA complex disassembly	0.006	SMARCE1	1
cellular response to prostaglandin stimulus	0.007	PRKCE	1
calcium ion transport	0.007	PRKCE/FGF2	2
uronic acid metabolic process	0.007	PRKCE	1
glucuronate metabolic process	0.007	PRKCE	1
regulation of lipid metabolic process	0.007	PRKCE/FGF2	2
response to prostaglandin E	0.008	PRKCE	1
positive regulation of vascular endothelial cell proliferation	0.008	FGF2	1
regulation of endothelial cell chemotaxis	0.008	FGF2	1
cellular calcium ion homeostasis	0.008	PRKCE/FGF2	2
exploration behavior	0.008	PRKCE	1
negative regulation of fibroblast growth factor receptor signaling pathway	0.008	FGF2	1
positive regulation of lipid catabolic process	0.009	PRKCE	1
calcium ion homeostasis	0.009	PRKCE/FGF2	2
divalent metal ion transport	0.009	PRKCE/FGF2	2
inositol phosphate biosynthetic process	0.009	FGF2	1
divalent inorganic cation transport	0.009	PRKCE/FGF2	2
ameboidal-type cell migration	0.009	PRKCE/FGF2	2
cellular divalent inorganic cation homeostasis	0.009	PRKCE/FGF2	2
response to isoquinoline alkaloid	0.010	PRKCE	1
response to morphine	0.010	PRKCE	1
response to prostaglandin	0.010	PRKCE	1
endothelial cell chemotaxis	0.010	FGF2	1
positive regulation of phosphatidylinositol 3-kinase activity	0.010	FGF2	1
MyD88-independent toll-like receptor signaling pathway	0.011	PRKCE	1
regulation of synaptic transmission, GABAergic	0.011	PRKCE	1
lens fiber cell differentiation	0.011	FGF2	1
hyaluronan metabolic process	0.012	FGF2	1
secretion by tissue	0.012	PRKCE	1
positive regulation of cell migration involved in sprouting angiogenesis	0.012	FGF2	1
positive regulation of lipid kinase activity	0.012	FGF2	1
positive regulation of cardiac muscle cell proliferation	0.012	FGF2	1

Table continued on next page.....

Description	P value	Gene	Count
regulation of cell fate commitment	0.012	FGF2	1
positive regulation of cytokinesis	0.013	PRKCE	1
toll-like receptor 4 signaling pathway	0.013	PRKCE	1
regulation of fibroblast growth factor receptor signaling pathway	0.013	FGF2	1
positive regulation of pri-miRNA transcription by RNA polymerase II	0.013	FGF2	1
positive regulation of phospholipase C activity	0.015	FGF2	1
synaptic transmission, GABAergic	0.015	PRKCE	1
positive regulation of cardiac muscle tissue growth	0.015	FGF2	1
regulation of phospholipase C activity	0.015	FGF2	1
vascular endothelial cell proliferation	0.016	FGF2	1
positive regulation of phospholipid metabolic process	0.016	FGF2	1
positive regulation of vascular associated smooth muscle cell proliferation	0.016	FGF2	1
regulation of vascular endothelial cell proliferation	0.016	FGF2	1
regulation of pri-miRNA transcription by RNA polymerase II	0.016	FGF2	1
regulation of blood vessel endothelial cell proliferation involved in sprouting angiogenesis	0.016	FGF2	1
positive regulation of heart growth	0.016	FGF2	1
negative regulation of fat cell differentiation	0.017	RUNX1T1	1
pri-miRNA transcription by RNA polymerase II	0.017	FGF2	1
regulation of sodium ion transmembrane transporter activity	0.017	PRKCE	1
regulation of insulin secretion involved in cellular response to glucose stimulus	0.018	PRKCE	1
cellular response to fatty acid	0.018	PRKCE	1
blood vessel endothelial cell proliferation involved in sprouting angiogenesis	0.018	FGF2	1
regulation of phosphatidylinositol 3-kinase activity	0.018	FGF2	1
branching involved in ureteric bud morphogenesis	0.019	FGF2	1
lipopolysaccharide-mediated signaling pathway	0.019	PRKCE	1
regulation of cardiac muscle cell proliferation	0.019	FGF2	1
regulation of lipid catabolic process	0.019	PRKCE	1
glycosaminoglycan catabolic process	0.019	FGF2	1
positive regulation of wound healing	0.019	PRKCE	1
positive regulation of protein localization to plasma membrane	0.019	PRKCE	1
positive regulation of phospholipase activity	0.020	FGF2	1
positive regulation of cellular carbohydrate metabolic process	0.020	PRKCE	1
positive regulation of cardiac muscle tissue development	0.020	FGF2	1
positive regulation of organ growth	0.020	FGF2	1
polyol biosynthetic process	0.020	FGF2	1
insulin secretion involved in cellular response to glucose stimulus	0.020	PRKCE	1
ureteric bud morphogenesis	0.020	FGF2	1
regulation of sodium ion transmembrane transport	0.020	PRKCE	1
mesonephric tubule morphogenesis	0.021	FGF2	1
aminoglycan catabolic process	0.021	FGF2	1
regulation of lipid kinase activity	0.021	FGF2	1

Table continued on next page.....

Description	P value	Gene	Count
positive chemotaxis	0.021	FGF2	1
positive regulation of sprouting angiogenesis	0.021	FGF2	1
positive regulation of protein localization to cell periphery	0.021	PRKCE	1
cardiac muscle cell proliferation	0.022	FGF2	1
positive regulation of DNA biosynthetic process	0.022	FGF2	1
inositol phosphate metabolic process	0.023	FGF2	1
regulation of phospholipase activity	0.023	FGF2	1
nephron tubule morphogenesis	0.023	FGF2	1
positive regulation of insulin secretion	0.023	PRKCE	1
positive regulation of response to wounding	0.023	PRKCE	1
positive regulation of epithelial cell differentiation	0.024	FGF2	1
somatic stem cell population maintenance	0.024	FGF2	1
nephron epithelium morphogenesis	0.024	FGF2	1
positive regulation of lipase activity	0.024	FGF2	1
negative regulation of ion transmembrane transporter activity	0.024	PRKCE	1
renal tubule morphogenesis	0.024	FGF2	1
nephron morphogenesis	0.024	FGF2	1
negative regulation of wound healing	0.025	FGF2	1
positive regulation of blood vessel endothelial cell migration	0.025	FGF2	1
negative regulation of protein ubiquitination	0.025	PRKCE	1
regulation of cardiac muscle tissue growth	0.025	FGF2	1
regulation of release of sequestered calcium ion into cytosol	0.025	PRKCE	1
lens development in camera-type eye	0.026	FGF2	1
striated muscle cell proliferation	0.026	FGF2	1
positive regulation of carbohydrate metabolic process	0.026	PRKCE	1
positive regulation of striated muscle tissue development	0.027	FGF2	1
positive regulation of muscle organ development	0.027	FGF2	1
positive regulation of muscle tissue development	0.027	FGF2	1
regulation of heart growth	0.027	FGF2	1
regulation of cell migration involved in sprouting angiogenesis	0.027	FGF2	1
regulation of vascular associated smooth muscle cell proliferation	0.027	FGF2	1
vascular associated smooth muscle cell proliferation	0.027	FGF2	1
regulation of sodium ion transport	0.028	PRKCE	1
negative regulation of transporter activity	0.028	PRKCE	1
negative regulation of blood vessel endothelial cell migration	0.028	FGF2	1
regulation of cytokinesis	0.028	PRKCE	1
ATP-dependent chromatin remodeling	0.028	SMARCE1	1
response to fatty acid	0.028	PRKCE	1
cellular response to alcohol	0.029	PRKCE	1
negative regulation of cation transmembrane transport	0.029	PRKCE	1
negative regulation of protein modification by small protein conjugation or removal	0.029	PRKCE	1

Table continued on next page.....

Description	P value	Gene	Count
nephron tubule development	0.029	FGF2	1
negative regulation of response to wounding	0.029	FGF2	1
kidney morphogenesis	0.030	FGF2	1
carbohydrate derivative transport	0.030	PRKCE	1
body fluid secretion	0.030	PRKCE	1
renal tubule development	0.030	FGF2	1
regulation of phospholipid metabolic process	0.030	FGF2	1
cellular response to ketone	0.030	PRKCE	1
ureteric bud development	0.031	FGF2	1
mesonephric epithelium development	0.031	FGF2	1
mesonephric tubule development	0.031	FGF2	1
positive regulation of peptide hormone secretion	0.031	PRKCE	1
cell fate specification	0.032	FGF2	1
regulation of calcium ion transport into cytosol	0.032	PRKCE	1
positive regulation of actin filament polymerization	0.032	PRKCE	1
macrophage activation	0.032	PRKCE	1
regulation of lipase activity	0.032	FGF2	1
regulation of cardiac muscle tissue development	0.032	FGF2	1
regulation of protein localization to plasma membrane	0.032	PRKCE	1
mesonephros development	0.032	FGF2	1
cell migration involved in sprouting angiogenesis	0.032	FGF2	1
negative regulation of ion transmembrane transport	0.032	PRKCE	1
positive regulation of smooth muscle cell proliferation	0.032	FGF2	1
response to alkaloid	0.033	PRKCE	1
negative regulation of endothelial cell migration	0.034	FGF2	1
cardiac muscle tissue growth	0.034	FGF2	1
regulation of DNA biosynthetic process	0.034	FGF2	1
nephron epithelium development	0.034	FGF2	1
positive regulation of endothelial cell proliferation	0.035	FGF2	1
mucopolysaccharide metabolic process	0.035	FGF2	1
heart growth	0.036	FGF2	1
regulation of organ growth	0.036	FGF2	1
phosphatidylinositol biosynthetic process	0.037	FGF2	1
fibroblast growth factor receptor signaling pathway	0.037	FGF2	1
positive regulation of cell-substrate adhesion	0.038	PRKCE	1
response to ethanol	0.038	PRKCE	1
regulation of protein localization to cell periphery	0.038	PRKCE	1
negative regulation of epithelial cell migration	0.039	FGF2	1
positive regulation of protein localization to membrane	0.040	PRKCE	1
negative regulation of transmembrane transport	0.040	PRKCE	1
stem cell proliferation	0.040	FGF2	1

Table continued on next page.....

Description	P value	Gene	Count
positive regulation of hormone secretion	0.041	PRKCE	1
positive regulation of endothelial cell migration	0.041	FGF2	1
polyol metabolic process	0.041	FGF2	1
cellular response to glucose stimulus	0.042	PRKCE	1
cellular response to hexose stimulus	0.042	PRKCE	1
positive regulation of protein polymerization	0.043	PRKCE	1
cellular response to monosaccharide stimulus	0.043	PRKCE	1
immune response-regulating cell surface receptor signaling pathway involved in phagocytosis	0.043	PRKCE	1
Fc-gamma receptor signaling pathway involved in phagocytosis	0.043	PRKCE	1
Fc-gamma receptor signaling pathway	0.044	PRKCE	1
kidney epithelium development	0.044	FGF2	1
regulation of fat cell differentiation	0.045	RUNX1T1	1
nephron development	0.045	FGF2	1
positive regulation of chemotaxis	0.045	FGF2	1
Fc receptor mediated stimulatory signaling pathway	0.045	PRKCE	1
cellular response to carbohydrate stimulus	0.045	PRKCE	1
cellular response to fibroblast growth factor stimulus	0.046	FGF2	1
regulation of cellular carbohydrate metabolic process	0.046	PRKCE	1
regulation of sprouting angiogenesis	0.046	FGF2	1
Golgi organization	0.047	TMED5	1
toll-like receptor signaling pathway	0.047	PRKCE	1
regulation of calcium ion transmembrane transport	0.047	PRKCE	1
cellular glucose homeostasis	0.048	PRKCE	1
regulation of striated muscle tissue development	0.048	FGF2	1
response to fibroblast growth factor	0.048	FGF2	1
positive regulation of small molecule metabolic process	0.048	PRKCE	1
branching morphogenesis of an epithelial tube	0.048	FGF2	1
activation of MAPK activity	0.049	FGF2	1
regulation of muscle tissue development	0.049	FGF2	1
negative regulation of ion transport	0.049	PRKCE	1
regulation of muscle organ development	0.049	FGF2	1
platelet activation	0.049	PRKCE	1
glycosaminoglycan metabolic process	0.049	FGF2	1
npBAF complex	0.004	SMARCE1	1
nBAF complex	0.005	SMARCE1	1
SWI/SNF complex	0.007	SMARCE1	1
endoplasmic reticulum exit site	0.012	TMED5	1
cis-Golgi network	0.025	TMED5	1
sarcoplasmic reticulum	0.025	CALU	1
SWI/SNF superfamily-type complex	0.026	SMARCE1	1
endoplasmic reticulum-Golgi intermediate compartment membrane	0.027	TMED5	1

Table continued on next page.....

Description	P value	Gene	Count
ATPase complex	0.028	SMARCE1	1
sarcoplasm	0.028	CALU	1
COPII-coated ER to Golgi transport vesicle	0.034	TMED5	1
melanosome	0.037	CALU	1
pigment granule	0.037	CALU	1
nuclear matrix	0.038	RUNX1T1	1
endoplasmic reticulum-Golgi intermediate compartment	0.046	TMED5	1
nuclear periphery	0.046	RUNX1T1	1
transcription coregulator activity	0.001	FGF2/ SMARCE1/ RUNX1T1	3
transcription coactivator activity	0.004	FGF2/ SMARCE1	2
protein kinase C activity	0.006	PRKCE	1
calcium-dependent protein kinase C activity	0.006	PRKCE	1
calcium-dependent protein serine/threonine kinase activity	0.009	PRKCE	1
calcium-dependent protein kinase activity	0.009	PRKCE	1
fibroblast growth factor receptor binding	0.009	FGF2	1
actin monomer binding	0.011	PRKCE	1
14-3-3 protein binding	0.012	PRKCE	1
chemokine binding	0.013	FGF2	1
signaling receptor activator activity	0.014	PRKCE/FGF2	2
chemoattractant activity	0.014	FGF2	1
nucleosomal DNA binding	0.015	SMARCE1	1
nuclear receptor transcription coactivator activity	0.020	FGF2	1
nucleosome binding	0.026	SMARCE1	1
N-acetyltransferase activity	0.032	SMARCE1	1
alcohol binding	0.032	PRKCE	1
nuclear receptor binding	0.038	SMARCE1	1
acetyltransferase activity	0.039	SMARCE1	1
chromatin DNA binding	0.040	SMARCE1	1
N-acyltransferase activity	0.040	SMARCE1	1

GO, Gene Ontology.